

Numerical Solution of a 3D System of Transient and Nonlinear PDEs Arising from Larvae-Algae-Mussels Interactions

Ramoni Z. S. Azevedo[1], Charles H. X. B. Barbosa[2], Isaac P. Santos[1,3(✉)], José C. R. Silva[4], Dayse H. Pastore[4], Anna R. C. Costa[4], Claudia M. Dias[2], Raquel M. A. Figueira[5], and Humberto F. M. Fortunato[5]

[1] Federal University of Espírito Santo, Vitória, Espírito Santo, Brazil
ramoni.sedano@aluno.ufes.br
[2] Federal Rural University of Rio de Janeiro, Seropédica, Rio de Janeiro, Brazil
mazza@ufrrj.br
[3] Federal University of Espírito Santo, São Mateus, Espírito Santo, Brazil
isaac.santos@ufes.br
[4] Federal Centers of Technical Education Celso Suckow da Fonseca, Rio de Janeiro, Rio de Janeiro, Brazil
{jose.rubianes,dayse.pastore,anna.costa}@cefet-rj.br
[5] hubz, Rio de Janeiro, Rio de Janeiro, Brazil
{raquel.figueira,humberto.fortunato}@hubz.com.br

Abstract. In this work we present a numerical solution of a 3D system of transient and nonlinear partial differential equations. The model arises from larvae, algae and mussel interactions, which takes place in the Pereira Barreto channel, connecting an important Brazilian hydroelectric plant to a river. The mathematical model, proposed in Silva [1] for the two-dimensional case, is composed of three advective-diffusive-reactive equations for species densities coupled with the Navier-Stokes equations to simulate the velocity field of the channel. A numerical discretization of the model is proposed within the framework of the finite element method. Since the problem is advection-dominated, we resort to the well-known stabilization schemes, SUPG and CAU, to obtain oscillations-free solutions. The spatial discretization produces a fully implicit set of nonlinear differential algebraic equations that is integrated numerically in time by the two-step Backward Differentiation Formula of second order, whereas the nonlinear process is solved by a Picard fixed point iteration. The proposed formulation is used to simulate the dynamics of species proliferation and to quantify the golden mussel population in a stretch of the Pereira Barreto channel, with a focus on population control measures. The preliminary results, as well as other considerations related to the problem and the numerical model, are discussed.

Keywords: Larvae-Algae-Mussel model · Numerical method · Nonlinear system of PDEs

© The Author(s), under exclusive license to Springer Nature Switzerland AG 2022
O. Gervasi et al. (Eds.): ICCSA 2022 Workshops, LNCS 13377, pp. 684–697, 2022.
https://doi.org/10.1007/978-3-031-10536-4_45

1 Introduction

The presence of golden mussel (*Limnoperna fortunei* (Dunker, 1857)) in Brazil is considered an environmental problem of great concern today. The Brazilian Institute for the Environment and Renewable Natural Resources (IBAMA) classifies the golden mussel as one of the three priority invasive species for control, since its overpopulation can cause serious problems for the native fauna [2]. It is a small freshwater bivalve mollusk, commonly known as the golden mussel due to its yellowish shell. This is a filter feeding species with a capacity to filter more than its own weight in microalgae per hour [3]. The animal has external reproduction, releasing gametes in the water which then produce planktonic larvae that can be carried by water currents for up to 10–20 days [4]. After this period, the mussel will go through recruitment in which the larvae will seek a proper substrate for attachment and will form a byssus for permanent fixation on the selected spot. Originating in China with its high tolerance to different environments and counting on human assistance in its transport, this species adapted well to Brazilian rivers, and is a threat even to the Amazonian aquatic ecosystems, which hold the largest and still unknown aquatic biodiversity in the world.

It is known that the areas invaded by the mussel undergo significant modifications [5], especially in environments already affected by human activity such as hydroelectric power plant reservoirs. In these areas, the animals can block the grids, pipes and heat exchangers, a particularly favored spot where the temperature contributes to the reproduction and growth of the bivalve.

Mathematical modeling is a very useful tool in the study of the relationship between biological species and their environment, having the ability to efficiently integrate and evaluate multiple complex processes simultaneously, helping to understand biological phenomena. In [1] is presented a mathematical model combining hydrodynamics and populational dynamics to simulate the distribution of mussels considering a two-dimensional geometry of the reservoir of the Três Irmãos Hydroelectric Power Plant (HPP), in Brazil.

The good results obtained by the model in two-dimensional experiments motivated us to evaluate its behavior in a three-dimensional domain. Thus, in this work we present a 3D numerical formulation, based on the finite element method, for the model described in [1], with the aim of analyze the mussel infestation in a stretch of the Pereira Barreto channel, located in the municipality of the same name in the state of São Paulo. The channel is the second largest artificial freshwater channel in the world, $9,600\,\mathrm{m}$ long, bottom width variable between 50 and 70 m, 12 m deep at the height upstream and 8 m at the minimum level and maximum flow of $1,600\,\mathrm{m}^3/\mathrm{s}$. It makes the hydraulic interconnection of the reservoirs of the Três Irmãos and Ilha Solteira HPPs, and enabling the optimization of energy generation electricity in these plants and the navigation between the north and south stretches of the Paraná waterway and the connection to the north stretch of the Paraná waterway with Tietê waterway. In this way, the channel became a propagation medium for the golden mussel between the Tietê and São José dos Dourados rivers.

The mathematical model is composed of two advective-diffusive-reactive equations for larvae and algae densities, one diffusive-reactive equation for mussels density, coupled with the unsteady incompressible Navier-Stokes equations. Since the problem is convection-dominated, we apply the Streamline Upwind Petrov Galerkin (SUPG) method to obtain global oscillations-free solutions [6], and the discontinuity capturing Consistent Approximate Upwind (CAU) scheme which represents boundary layers accurately [7,8]. The spatial discretization produces a fully implicit set of nonlinear differential algebraic equations that are integrated numerically in time by the two-step Backward Differentiation Formula of second order, whereas the nonlinear process is solved using Picard fixed point iteration.

The remainder of this work is organized as follows. The mathematical model is presented in Sect. 2. We present the numerical formulation in Sect. 3. Section 4 is devoted to numerical simulations and Sect. 5 concludes this paper.

2 Mathematical Model

Let $\Omega \subset \mathbb{R}^3$ be a bounded domain with a Lipschitz boundary Γ with an outward unit normal $\boldsymbol{n}$, and $[0, t_F]$ the temporal interval, with $t_F > 0$. Denoting by $L = L(\boldsymbol{x}, t)$, $M = M(\boldsymbol{x}, t)$ and $A = A(\boldsymbol{x}, t)$ the densities of larvae, mussels and algae, respectively, at $(\boldsymbol{x}, t) \in \Omega \times [0, t_F]$, the Larvae-Mussel-Algae model consists of finding L, M and A such that

$$\frac{\partial L}{\partial t} - D_L \Delta L + \boldsymbol{u} \cdot \boldsymbol{\nabla} L = r_1 M \left(1 - \frac{L}{K_L}\right) - (b_1 + \lambda_L) L, \text{ in } \Omega \times [0, t_F], \tag{1}$$

$$\frac{\partial M}{\partial t} - D_M \Delta M = \lambda_M \left(\frac{A^2}{c_1^2 + A^2}\right) L \left(1 - \frac{M}{K_M}\right) - b_2 M, \text{ in } \Omega_M \times [0, t_F], \tag{2}$$

$$\frac{\partial A}{\partial t} - D_A \Delta A + \boldsymbol{u} \cdot \boldsymbol{\nabla} A = r_2 A \left(1 - \frac{A}{K_A}\right) - b_3 \left(\frac{A^2}{c_2^2 + A^2}\right) M, \text{ in } \Omega \times [0, t_F]. \tag{3}$$

The mathematical model (1)–(3), with appropriate boundary and initial conditions, is presented in [1] to solve a two-dimensional problem for quantifying the population of golden mussels in HPP reservoirs. In the equation for larvae, Eq. (1), $D_L > 0$ is the diffusivity coefficient, r_1 is the intrinsic growth rate, K_L is the limiting factor, b_1 is the mortality rate and λ_L is the maturation rate, which represents the larvae that successfully turns into adult golden mussel. In the equation for mussels, Eq. (2), $D_M > 0$ is the diffusivity coefficient, K_M is the the carrying capacity, c_1 is half saturation constant for the adults, b_2 is the mortality rate due to fish predation, and λ_M is the maturation rate. In the equation for algae, Eq. (3), $D_A > 0$ is the diffusivity coefficient, K_A is the the carrying capacity, r_2 is the intrinsic growth rate, b_3 is the mortality rate due to predation by golden mussels, and c_2 is half saturation constant for algae; $\Omega_M \subset \Omega$ is the spatial domain for the mussels, representing a layer close to the boundary walls (solid substrates and side walls). For a better understanding of this model see [1].

Equations (1), (2) and (3) form a system of transient and nonlinear coupled partial differential equations which models advective-diffusive-reactive phenomenons. Advective terms appear in the larvae and algae equations, where the free divergence velocity field, $\boldsymbol{u}$, is obtained from the unsteady incompressible Navier-Stokes equations.

Dirichlet boundary conditions are imposed only for the mussel equation, that is,

$$M(\boldsymbol{x},t) = g_M^D(\boldsymbol{x}),\ \forall\ (\boldsymbol{x},t) \in \Gamma_M^D \times [0,t_F], \tag{4}$$

where Γ_M^D represents the Dirichlet boundary for the mussels and $g_M^D(\cdot)$ is a given function. Homogeneous Neumann boundary conditions are defined for the larvae and algae equations on Γ, that is,

$$D_L \boldsymbol{\nabla} L(\boldsymbol{x},t) \cdot \boldsymbol{n}(\boldsymbol{x}) = 0,\ \forall\ (\boldsymbol{x},t) \in \Gamma^N \times [0,t_F], \tag{5}$$

$$D_A \boldsymbol{\nabla} A(\boldsymbol{x},t) \cdot \boldsymbol{n}(\boldsymbol{x}) = 0,\ \forall\ (\boldsymbol{x},t) \in \Gamma^N \times [0,t_F], \tag{6}$$

where $\Gamma^N \subset \Gamma$ is the part of the boundary with Neumann conditions. The homogeneous Neumann boundary condition means that there is no population movement of larvae and algae across the boundary, Γ. The mathematical model (1)–(3) is completed by assuming the initial conditions,

$$L(\boldsymbol{x},0) = L_0(\boldsymbol{x}), \quad M(\boldsymbol{x},0) = M_0(\boldsymbol{x}), \quad A(\boldsymbol{x},0) = A_0(\boldsymbol{x}), \tag{7}$$

where L_0, M_0, A_0 are given functions representing the initial densities of larvae, mussels and algae, respectively.

In order to describe the variational formulation of this problem we define the following function spaces, $V_L = V_A = H^1(\Omega)$ and

$$V_M = \{w \in H^1(\Omega_M);\ w_h = g_M^D \text{ on } \Gamma_M^D\}, \tag{8}$$

where $H^1(\Omega)$ is the Sobolev space consisting of functions for which all partial derivatives up to order one are square integrables in Ω; V_L, V_M, V_A are function spaces associated with the equations for larvae, mussels and algae, respectively. Thus, for $t \in [0,t_F]$, the variational formulation of (1)–(3) consists of finding $(L,M,A) \in V_L \times V_M \times V_A$ such that

$$\left(\frac{\partial L}{\partial t}, v_L\right) + D_L(\boldsymbol{\nabla} L, \boldsymbol{\nabla} v_L) + (\boldsymbol{u} \cdot \boldsymbol{\nabla} L, v_L) + (\sigma_L L, v_L) = (f_L, v_L), \tag{9}$$

$$\left(\frac{\partial M}{\partial t}, v_M\right) + D_M(\boldsymbol{\nabla} M, \boldsymbol{\nabla} v_M) + (\sigma_M M, v_M) = (f_M, v_M), \tag{10}$$

$$\left(\frac{\partial A}{\partial t}, v_A\right) + D_A(\boldsymbol{\nabla} A, \boldsymbol{\nabla} v_A) + (\boldsymbol{u} \cdot \boldsymbol{\nabla} A, v_A) + (\sigma_A A, v_A) = (f_A, v_A), \tag{11}$$

for all $v_L \in V_L$, $v_A \in V_A$, and $v_M \in V_M^0 = \{w \in H^1(\Omega);\ w_h = 0 \text{ on } \Gamma_M^D\}$, where

$$\sigma_L = \sigma_L(M) = \left(\lambda_L + b_1 + \frac{r_1}{K_L}M\right), \quad f_L = f_L(M) = r_1 M,$$

$$\sigma_M = \sigma_M(A, L) = \left[b_2 + \frac{\lambda_M}{K_M}\left(\frac{A^2}{c_1^2 + A^2}\right)L\right], \quad f_M = f_M(A, L) = \lambda_M\left(\frac{A^2}{c_1^2 + A^2}\right)L,$$

$$\sigma_A = \sigma_A(A, M) = \left[b_3\left(\frac{AM}{c_2^2 + A^2}\right) + \frac{r_2 A}{K_A}\right], \quad f_A = f_A(A) = r_2 A.$$

The velocity field $\boldsymbol{u}$ in the advective terms of (1) and (3) is obtained from the unsteady incompressible Navier-Stokes equations, given by

$$\frac{\partial \boldsymbol{u}}{\partial t} + (\boldsymbol{u} \cdot \boldsymbol{\nabla})\boldsymbol{u} - \nu \Delta \boldsymbol{u} + \boldsymbol{\nabla} p = \boldsymbol{f},\ \forall\ (\boldsymbol{x}, t) \in \Omega \times [0, t_F], \tag{12}$$

$$\boldsymbol{\nabla} \cdot \boldsymbol{u} = 0,\ \forall\ (\boldsymbol{x}, t) \in \Omega \times [0, t_F], \tag{13}$$

$$\boldsymbol{u} = \boldsymbol{0},\ \forall\ (\boldsymbol{x}, t) \in \Gamma_{\boldsymbol{u}}^D \times [0, t_F], \tag{14}$$

$$\boldsymbol{u} = \boldsymbol{g}_{\boldsymbol{u}}^D,\ \forall\ (\boldsymbol{x}, t) \in \Gamma_{\boldsymbol{u}}^{D,in} \times [0, t_F], \tag{15}$$

$$\boldsymbol{u}(\boldsymbol{x}, 0) = \boldsymbol{u}_0(\boldsymbol{x}),\ \forall\ \boldsymbol{x} \in \Omega, \tag{16}$$

where p is the rate between the pressure and the density, ν is the kinematic viscosity (constant), $\boldsymbol{f}$ is a given external force field per unit mass, $\boldsymbol{u}_0(\cdot)$ is the initial velocity, $\boldsymbol{g}_{\boldsymbol{u}}^D$ is a known function defined on the Dirichlet inflow boundary, $\Gamma_{\boldsymbol{u}}^{D,in} = \{\boldsymbol{x} \in \Gamma;\ \boldsymbol{u} \cdot \boldsymbol{n} \leq 0\}$, and $\Gamma_{\boldsymbol{u}}^D = \Gamma \setminus (\Gamma_{\boldsymbol{u}}^{D,in} \cup \Gamma_{\boldsymbol{u}}^{D,out})$. The Navier-Stokes model was solved by the Characteristic Galerkin method [9].

3 Numerical Formulation

In this section we present a numerical formulation for solving the system (1)–(3) based on the finite element method [9–11].

We consider a regular partition $\mathcal{T}_h = \{K\}$ of the domain $\Omega \subset \mathbb{R}^3$ into tetrahedral elements, where h stands for the mesh size. The finite dimensional spaces associated to V_L, V_M, V_A, V_M^0 are denoted by $V_{h,\alpha}$, $\alpha \in \{L, M, A\}$, and $V_{h,M}^0$, respectively, and defined as

$$V_{h,\alpha} = \{w_h \in H^1(\Omega) : w_h|_K \in \mathbb{P}_1(K),\ \forall K \in \mathcal{T}_h\},\ \alpha \in L, A, \tag{17}$$

$$V_{h,M} = \{w_h \in H^1(\Omega_M) : w_h|_K \in \mathbb{P}_1(K),\ \forall K \in \mathcal{T}_h,\ w_h = g_M^D \text{ on } \Gamma_M^D\}, \tag{18}$$

$$V_{h,M}^0 = \{w_h \in H^1(\Omega) : w_h|_K \in \mathbb{P}_1(K),\ \forall K \in \mathcal{T}_h,\ w_h = 0 \text{ on } \Gamma_M^D\}, \tag{19}$$

where $\mathbb{P}_1(K)$ is the set of first order polynomials defined in K.

We approximate the time derivatives by the two-step Backward Differentiation Formula of order 2 (BDF2) [12],

$$\tilde{\mathcal{D}}_{\Delta t}^{\alpha,k+1} = \frac{3\alpha^{k+1} - 4\alpha^k + \alpha^{k-1}}{2\Delta t}, \quad \alpha \in \{L, M, A\}. \tag{20}$$

The BDF2 method is one of the most popular time-stepping methods for solving unsteady problems, due to its good stability property [12]. For the sake of presentation simplicity, we omit the subscript h for functions of the finite dimensional spaces. The numerical solution of (9)–(11) at time t_{k+1} consists of finding $(L^{k+1}, M^{k+1}, A^{k+1}) \in V_{h,L} \times V_{h,M} \times V_{h,A}$ such that

$$
\begin{aligned}
(\tilde{\mathcal{D}}_{\Delta t}^{L,k+1}, v_L) + D_L(\boldsymbol{\nabla} L, \boldsymbol{\nabla} v_L^{k+1}) + (\boldsymbol{u} \cdot \boldsymbol{\nabla} L^{k+1}, v_L) + (\sigma_L^{k+1} L^{k+1}, v_L) &= (f_L^{k+1}, v_L), \\
(\tilde{\mathcal{D}}_{\Delta t}^{M,k+1}, v_M) + D_M(\boldsymbol{\nabla} M^{k+1}, \boldsymbol{\nabla} v_M) + (\sigma_M^{k+1} M^{k+1}, v_M) &= (f_M^{k+1}, v_M), \\
(\tilde{\mathcal{D}}_{\Delta t}^{A,k+1}, v_A) + D_A(\boldsymbol{\nabla} A^{k+1}, \boldsymbol{\nabla} v_A) + (\boldsymbol{u} \cdot \boldsymbol{\nabla} A^{k+1}, v_A) + \left(\sigma_A^{k+1} A^{k+1}, v_A\right) &= (f_A^{k+1}, v_A),
\end{aligned}
$$

for all $(v_L, v_M, v_A) \in V_{h,L} \times V_{h,M}^0 \times V_{h,A}$.

The resulting system of nonlinear equations is solved by a Picard fixed point iteration. A numerical solution for L^{k+1}, M^{k+1} e A^{k+1} can be obtained by performing several iterations in the following way: for $s = 1, \cdots, s_{max}$, solve the system

$$
\begin{aligned}
\frac{3}{2\Delta t}(\tilde{L}^{s+1}, v_L) + D_L(\boldsymbol{\nabla} \tilde{L}^{s+1}, \boldsymbol{\nabla} v_L) + (\boldsymbol{u} \cdot \boldsymbol{\nabla} \tilde{L}^{s+1}, v_L) + (\tilde{\sigma}_L^s \tilde{L}^{s+1}, v_L) &= (\tilde{f}_L^s, v_L) \\
&\quad + \frac{2}{\Delta t}(L^k, v_L) - \frac{1}{2\Delta t}(L^{k-1}, v_L), \\
\frac{3}{2\Delta t}(\tilde{M}^{s+1}, v_M) + D_M(\boldsymbol{\nabla} \tilde{M}^{s+1}, \boldsymbol{\nabla} v_M) + (\tilde{\sigma}_M^s M^{k+1}, v_M) &= (\tilde{f}_M^s, v_M) \\
&\quad + \frac{2}{\Delta t}(M^k, v_M) - \frac{1}{2\Delta t}(M^{k-1}, v_L), \\
\frac{3}{2\Delta t}(\tilde{A}^{s+1}, v_A) + D_A(\boldsymbol{\nabla} \tilde{A}^{s+1}, \boldsymbol{\nabla} v_A) + (\boldsymbol{u} \cdot \boldsymbol{\nabla} \tilde{A}^{s+1}, v_A) + (\tilde{\sigma}_A^s \tilde{A}^{s+1}, v_A) &= (\tilde{f}_A, v_A) \\
&\quad + \frac{2}{\Delta t}(A^k, v_A) - \frac{1}{2\Delta t}(A^{k-1}, v_L),
\end{aligned}
\tag{21}
$$

where $\tilde{L}^{s+1}, \tilde{M}^{s+1}$ and $\tilde{L}^{s+1}$ are approximations of L^{k+1}, M^{k+1} and L^{k+1}, respectively; $\tilde{\sigma}_L^s = \sigma_L(\tilde{M}^s)$, $\tilde{f}_L = f_L(\tilde{M}^s)$, $\tilde{\sigma}_M^s = \sigma_M(\tilde{A}^s, \tilde{L}^s)$, $\tilde{f}_M^s = f_M(\tilde{A}^s, \tilde{L}^s)$, $\tilde{\sigma}_A^s = \sigma_A(\tilde{A}^s, \tilde{M}^s)$ and $\tilde{f}_A = f_A(\tilde{A}^s)$; s denotes the index of nonlinear iterations for each time (fixed) t_k. We insert in the model (21) two more terms inherent to the SUPG and CAU methods: the term

$$
\sum_{K \in \mathcal{T}_h} \left(R_L(\tilde{L}^{s+1}), \tau_{supg}^L \ \boldsymbol{u} \cdot \boldsymbol{\nabla} v_L\right)_K + \sum_{K \in \mathcal{T}_h} \left(\xi_{cau}^L(\tilde{L}^s) \boldsymbol{\nabla} \tilde{L}^{s+1}, \boldsymbol{\nabla} v_L\right)_K \tag{22}
$$

in the lef hand side of the first equation, and

$$
\sum_{K \in \mathcal{T}_h} \left(R_A(\tilde{A}^{s+1}), \tau_{supg}^A \ \boldsymbol{u} \cdot \boldsymbol{\nabla} v_A\right)_K + \sum_{K \in \mathcal{T}_h} \left(\xi_{cau}^A(\tilde{A}^s) \boldsymbol{\nabla} \tilde{A}^{s+1}, \boldsymbol{\nabla} v_A\right)_K \tag{23}
$$

in the left hand side of the third one, so that the dominant advection property of the model is well represented. In (22) and (23), $R_L(\cdot)$ and $R_A(\cdot)$ are the residuals of the larvae and algae equations, respectively, given by

$$
\begin{aligned}
R_L(\tilde{L}^{s+1}) &= \frac{3\tilde{L}^{s+1} - 4L^k + L^{k-1}}{2\Delta t} - D_L \Delta \tilde{L}^{s+1} + \boldsymbol{u} \cdot \boldsymbol{\nabla} \tilde{L}^{s+1} + \tilde{\sigma}_L^s \tilde{L}^{s+1} - \tilde{f}_L^s, \\
R_A(\tilde{A}^{s+1}) &= \frac{3\tilde{A}^{s+1} - 4A^k + A^{k-1}}{2\Delta t} - D_A \Delta \tilde{A}^{s+1} + \boldsymbol{u} \cdot \boldsymbol{\nabla} \tilde{A}^{s+1} + \tilde{\sigma}_A^s \tilde{A}^{s+1} - \tilde{f}_A^s,
\end{aligned}
$$

where τ^L_{supg} and τ^A_{supg} are the stabilization parameters of the SUPG method for the larvae and algae equations, respectively, whereas $\xi^L_{cau}(\cdot)$ and $\xi^A_{cau}(\cdot)$ are the nonlinear artificial diffusion functions of the CAU method for the larvae and algae equations. The definitions of τ^L_{supg}, τ^A_{supg}, $\xi^L_{cau}(\cdot)$ and $\xi^A_{cau}(\cdot)$ are found in [8].

4 Numerical Experiments

In this section we present the numerical experiments of this first approach for the solution of the proposed methodology. Our objective here is to understand if the solution obtained is close to the densities observed in the field. We used the FreeFem++ software [13] to generate the mesh and obtain the velocity field from the transient incompressible Navier-Stokes equations. A code in Matlab ©was developed to solve the system of partial differential equations, given in Eqs. (1)–(3). We considered a period of time of 4 months to evaluate the beginning of the golden mussel infestation. The 3D domain Ω represents a stretch of the Pereira Barreto channel, with 2 km long, close to the Três Irmãos HPP reservoir, located in the Tietê river basin, close to the municipalities of Pereira Barreto (SP) and Andradina (SP), shown in Fig. 1.

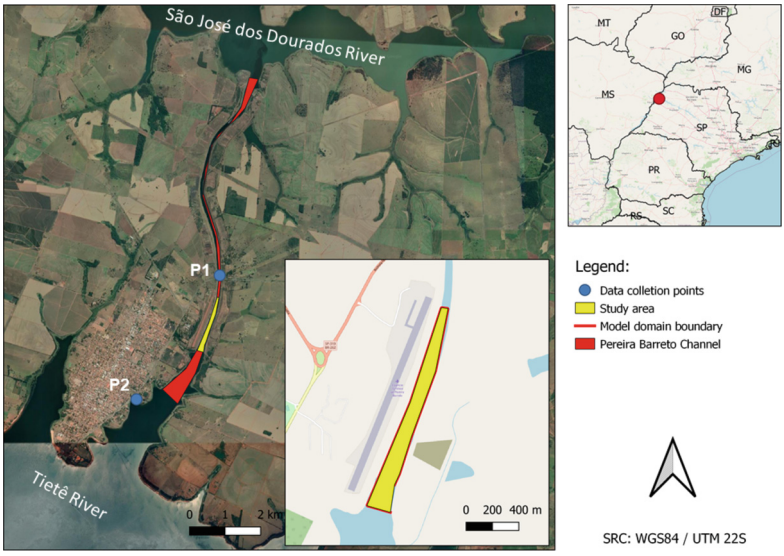

Fig. 1. Pereira barreto channel (adapted from google earth©).

The domain was discretized with 13,290 tetrahedral elements and 3,186 nodes, conforming mesh shown in Fig. 2. The following initial values were used for the populations: $L(\boldsymbol{x}, 0) = 0.0194115\ g/l$, $M(\boldsymbol{x}, 0) = 1\ g/m^3$ and

$A(\boldsymbol{x}, 0) = 0.001\ g/l$. First, we obtain the velocity field from the solution of the incompressible transient Navier-Stokes equations, using $\boldsymbol{u}_0 = \mathbf{0}$ in Ω, $\boldsymbol{g}_{\boldsymbol{u}}^{D} = 0.13\ m/s$ in $\Gamma_{\boldsymbol{u}}^{D,in}$ (channel inlet), and shown in Fig. 3. The parameters used in the simulations are describe in Table 1.

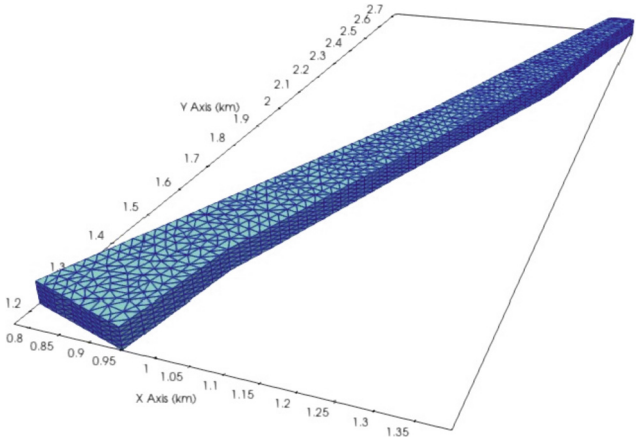

Fig. 2. Mesh used in the numerical experiments.

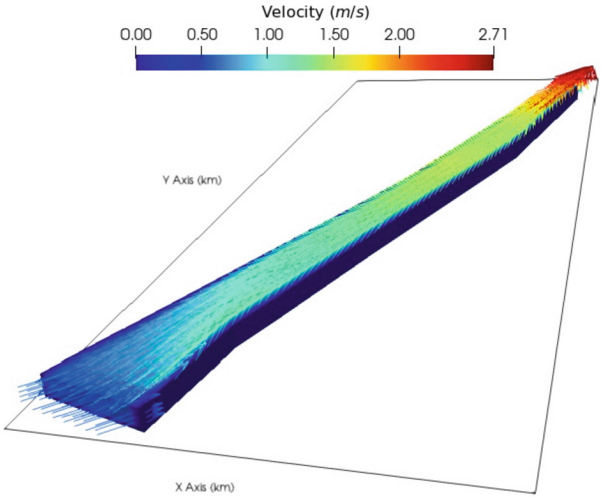

Fig. 3. Velocity field obtained from incompressible transient Navier-Stokes equations.

The solution at the first time step is obtained by the Backward Euler (BDF1) method since the BDF2 is a two-step scheme. Moreover, in each time step the algorithm performed $s_{max} = 20$ nonlinear steps. We carried out numerical simulations with and without the SUPG and CAU stabilized methods, and the importance of these formulations in the model became clear, providing numerical solutions without spurious oscillations and without negative values for the densities of the species.

Table 1. Parameters used in the numerical simulations.

Parameter	Value	Unit	Reference
D_A	1.2	m^2/day	(Cangelosi et al., 2015)
D_M	0.0012	m^2/day	(Montresor, 2014)
D_L	0.012	m^2/day	(Van de Koppel et al. 2005)
b_1	0.015	day^{-1}	Inferred
b_2	0.02	day^{-1}	Inferred
b_3	0.02	day^{-1}	Inferred
λ_M	0.03	day^{-1}	Inferred
λ_L	0.03	day^{-1}	Inferred
r_1	0.07	day^{-1}	Inferred
r_2	0.12	day^{-1}	Inferred
K_L	20	g/l	Inferred
K_M	$1,732$	g/m^3	Inferred
K_A	0.01	g/l	Inferred
c_1	0.001	g/l	Inferred
c_2	0.001	g/l	Inferred

Recent *in situ* measurements were carried out in December 2020 and August 2021, obtaining a mussel density of $3,936\ g/m^3$ and $7,546\ g/m^3$, respectively. It is worth mentioning that climatic and anthropic impacts were not included in the model. Below we present the evolution of the infestation over 4 months.

Figure 4 presents a logistical growth for the larvae population homogeneously throughout the channel for the first four months of infestation. As expected, this behavior follows the development of the adult mussel population (Fig. 5). However, we observed that in both cases the growth is slowed after third month. Finally, Fig. 6 shows a homogeneous behavior for the algae population throughout the section of the channel.

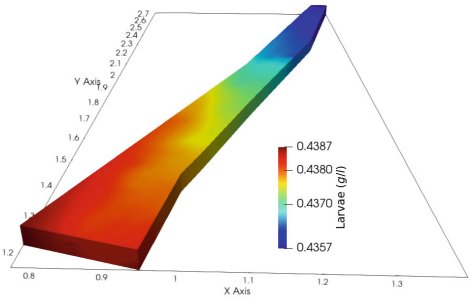

(a) 1 month

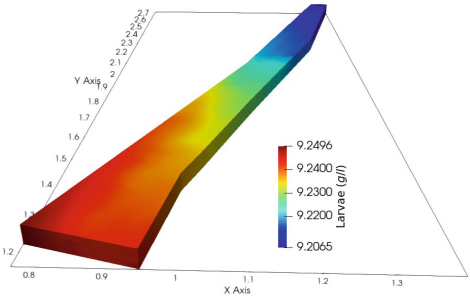

(b) 2 months

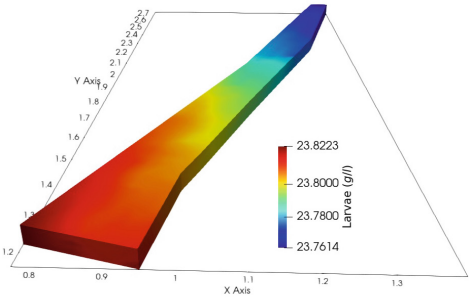

(c) 3 months

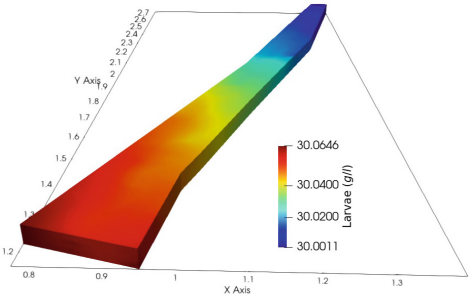

(d) 4 months

Fig. 4. Densities of Larvae after 4 months of infestation.

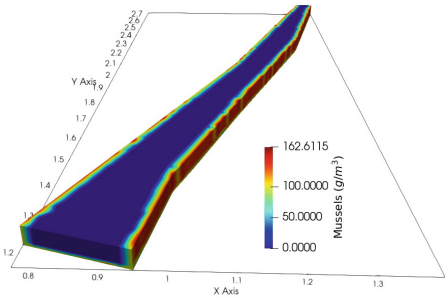

(a) 1 month

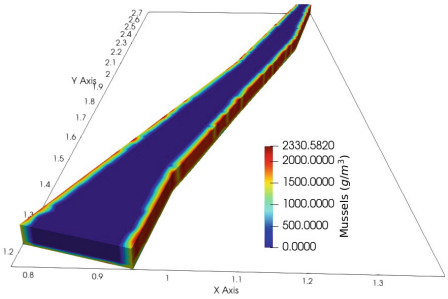

(b) 2 months

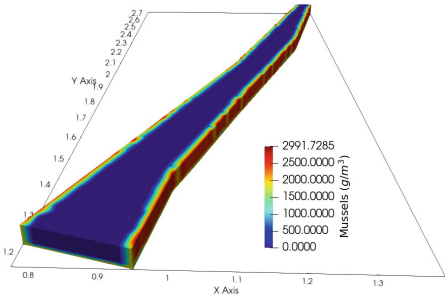

(c) 3 months

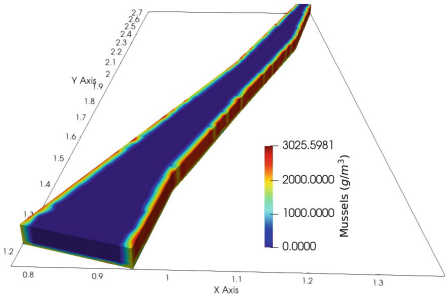

(d) 4 months

Fig. 5. Densities of Golden Mussels after 4 months of infestation.

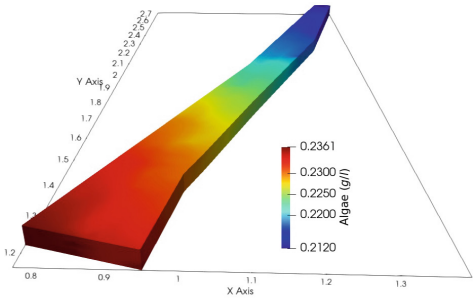

(a) 1 month

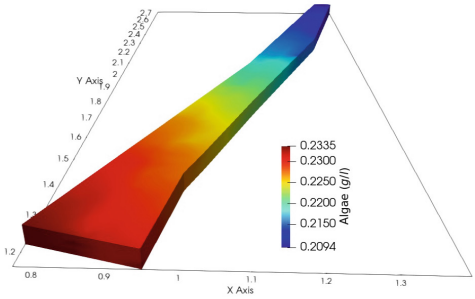

(b) 2 months

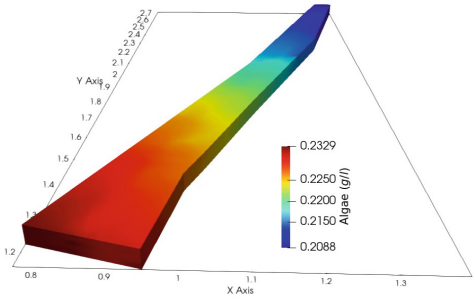

(c) 3 months

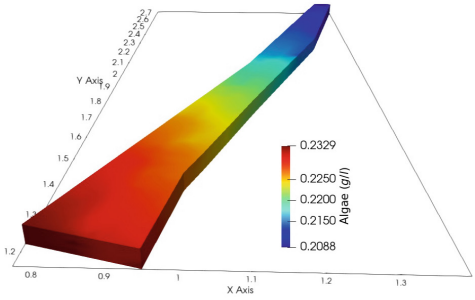

(d) 4 months

Fig. 6. Densities of Algae after 4 months of infestation.

5 Concluding Remarks

We presented a numerical formulation, based on the finite element method, for solving a complex 3D system of transient and nonlinear transport PDEs arising from larvae, algae and mussel interactions. The mathematical model is composed of three scalar transport equations for species densities coupled with the Navier-Stokes equations to simulate the velocity field of the channel. The numerical discretization of the model involves the use of the stabilized methods, SUPG and CAU. The fully implicit set of nonlinear differential algebraic equations is integrated numerically in time by the BDF2 scheme, whereas the nonlinear process is solved by a Picard fixed point iteration. The dynamics of the golden mussel population in their larvae and adult phases, and the algae population in a stretch of the channel, was observed through a preliminary numerical experiment that showed that the model represents well the interaction between the populations in the period of time evaluated. The analysis of the distribution of adult golden mussels corroborates the proposition that the Pereira Barreto channel has been serving as a nursery for the species, and that the infestation of the reservoir at Ilha Solteira HPP is mainly due to the arrival of larvae from the Três Irmãos HPP (already heavily infested), which through the channel, reach the São José dos Dourados river and then the Ilha Solteira HPP, thus forming a route for mussel infestation in the region.

Although this work has presented motivating results, this is a preliminary analysis and the simulations are in accordance with the dynamics recorded in the two-dimensional analysis [1]. A more complex computer simulation is being implemented, evaluating a longer period of time, using more refined meshes and a more extensive spatial domain in order to compare with the *in situ* data, and evaluate the convergence of the numerical process.

Acknowledgements. Research carried out within the scope of the project "Control of the Golden Mussel Infestation by Genetic Induction of Infertility" (PD-10381-0419/2019) with funding from CTG Brasil, SPIC Brasil and Tijoá Energia, within their ANEEL Research & Development Programs. This study was partially financed by the Coordenação de Aperfeiçoamento de Pessoal de Nível Superior - Brasil (CAPES) - Finance Code 001.

References

1. Silva, J.C.R., et al.: Population growth of the golden mussel (L. fortunei) in hydroelectric power plants: a study via mathematical and computational modeling. Braz. J. Water Res. **27** (2022). https://doi.org/10.1590/2318-0331.272220210124
2. IBAMA. Instituto Brasileiro do Meio Ambiente e dos Recursos Naturais Renováveis. Ministério do Meio Ambiente (2019). https://www.ibama.gov.br/especies-exoticas-invasoras/sobre-as-especies-exoticas-invasoras-sobre-especies-exoticas-invasoras. Accessed 31 Mar 2021
3. Sylvester, F., Dorado, J., Boltovskoy, D., Juarez, A., Cataldo, D.: Filtration rates of the invasive pest bivalve Limnoperna fortunei as a function of size and temperature. Hydrobiologia **534**, 71–80 (2005). https://doi.org/10.1007/s10750-004-1322-3

4. Cataldo, D., Boltovskoy, D., Hermosa, J., Canzi, C.: Temperature-dependent rates of larval development in limnoperna fortunei (bivalvia: mytilidae). J. Molluscan Stud. **71**(1), 41–46 (2005). https://doi.org/10.1093/mollus/eyi005
5. Karatayev, A., Burlakova, L., Padilla, D.: The effects of dreissena polymorpha (pallas) invasion on aquatic communities in Eastern Europe. J. Shellfish Res. **16**, 187–203 (1997)
6. Brooks, A.N., Hughes, T.J.R.: Streamline upwind Petrov-Galerkin formulations for convection dominated flows with particular emphasis on the incompressible Navier-Stokes equations. Comput. Methods Appl. Mech. Eng. **32**(1–3), 199–259 (1982)
7. Galeão, A.C., Dutra do Carmo, E.G.: A consistent approximate upwind Petrov-Galerkin method for convection-dominated problems. Comput. Methods Appl. Mech. Eng. **68**(1), 83–95 (1988)
8. Carmo, E.G.D., Alvarez, G.B.: A new stabilized finite element formulation for scalar convection-diffusion problems: the streamline and approximate upwind/Petrov-Galerkin method. Comput. Methods Appl. Mech. Eng. **192**(31–32), 3379–3396 (2003)
9. Donea, J., Huerta, A.: Finite Element Method for Flow Problems. Wiley, Oxford (2003)
10. Hughes, T.J.R.: The Finite Element Method: Linear Static and Dynamic Finite Element Analysis. Prentice-Hall International, Upper Saddle River (1987)
11. Roos, H., Stynes, M., Tobiska, L.: Robust Numerical Methods for Singularly Perturbed Differential Equations: Convection-Diffusion-Reaction and Flow Problems, 2nd edn. Springer, Heidelberg (2008). https://doi.org/10.1007/978-3-540-34467-4
12. Hairer, E., Norsett, S.P., Wanner, G.: Solving Ordinary Differential Equations. Springer Series in Computational Mathematics, 2nd edn. Springer, Heidelberg (2010). https://doi.org/10.1007/978-3-540-78862-1
13. Hecht, F.: New development in FreeFem++. J. Numer. Math. **20**(3–4), 251–266 (2012)